THE UNIVERSITY *of* EDINBURGH

Edinburgh Research Explorer

The MatP/matS Site-Specific System Organizes the Terminus Region of the E. coli Chromosome into a Macrodomain

OPEN ACCESS

The MatP/*matS* Site-Specific System Organizes the Terminus Region of the *E. coli* Chromosome into a Macrodomain

Romain Mercier,[1] Marie-Agnès Petit,[2] Sophie Schbath,[3] Stéphane Robin,[4] Meriem El Karoui,[2] Frédéric Boccard,[1,*] and Olivier Espéli[1,*]

[1]Centre de Génétique Moléculaire du CNRS, 91198 Gif-sur-Yvette, France
[2]INRA, UR888, Unité Bactéries Lactiques et Pathogènes Opportunistes, F-78350 Jouy-en-Josas, France
[3]INRA, UR1077 Mathématique, Informatique, et Génome, F-78350 Jouy-en-Josas, France
[4]AgroParisTech/INRA, UMR518 Unité Mathématiques et Informatique Appliquées, F-75005 Paris, France
*Correspondence: boccard@cgm.cnrs-gif.fr (F.B.), espeli@cgm.cnrs-gif.fr (O.E.)
DOI 10.1016/j.cell.2008.08.031

SUMMARY

The organization of the *Escherichia coli* chromosome into insulated macrodomains influences the segregation of sister chromatids and the mobility of chromosomal DNA. Here, we report that organization of the Terminus region (Ter) into a macrodomain relies on the presence of a 13 bp motif called *matS* repeated 23 times in the 800-kb-long domain. *matS* sites are the main targets in the *E. coli* chromosome of a newly identified protein designated MatP. MatP accumulates in the cell as a discrete focus that colocalizes with the Ter macrodomain. The effects of MatP inactivation reveal its role as main organizer of the Ter macrodomain: in the absence of MatP, DNA is less compacted, the mobility of markers is increased, and segregation of Ter macrodomain occurs early in the cell cycle. Our results indicate that a specific organizational system is required in the Terminus region for bacterial chromosome management during the cell cycle.

INTRODUCTION

The large size of genomes compared to cellular dimensions imposes extensive compaction of chromosomes compatible with DNA metabolism during replication, transcription, and segregation. Compaction of the chromosome results in the formation of a structure called the nucleoid. Work performed in different bacteria has revealed a number of processes involved in bacterial DNA condensation and organization; they include unrestrained DNA supercoiling, formation of a chromatin-like structure through the interaction of nucleoid-associated proteins (NAPs) with DNA, condensation by structural maintenance of chromosomes (SMC)-like proteins, and macromolecular crowding (Thanbichler and Shapiro, 2006). Cytological analyses have revealed that bacterial circular chromosomes are organized with a specific disposition within growing cells that preserves the linear order of loci in the

DNA (Viollier et al., 2004; Nielsen et al., 2006b; Wang et al., 2006). In *E. coli*, cytological (Niki et al., 2000) and genetic (Valens et al., 2004) analyses based on long distance DNA interactions revealed a structuring process that spatially insulates large regions of the chromosome called macrodomains (MDs). Collisions between DNA sites belonging to different MDs occur at low frequency, and two particular regions, called nonstructured (NS) regions, can interact with both flanking MDs (Valens et al., 2004). The Ori MD containing *oriC* is centered on *migS*, a centromere-like site involved in bipolar positioning of *oriC* (Yamaichi and Niki, 2004). Opposite the Ori MD, the Ter MD containing the replication terminus is centered on the chromosome dimer resolution site *dif*. The Ter MD is flanked by the Left and Right MDs, whereas the Ori MD is flanked by the two NS regions. MD organization was directly visualized by analysis of the positioning, the segregation pattern, and the dynamics of markers belonging to various MDs. Markers in MDs showed much lower mobility than markers in NS regions (Espéli et al., 2008).

Understanding of chromosome segregation has improved considerably in recent years (Thanbichler and Shapiro, 2006). Replication initiates from a single origin, *oriC*, and progresses bidirectionally to the terminus of replication located opposite the origin. In *E. coli*, replication initiation occurs in specific replication factories where both replisomes are colocalized. As replication progresses, foci representing the two replisomes follow separate paths (Bates and Kleckner, 2005; Reyes-Lamothe et al., 2008). A colocalization step between sister chromatids of the newly duplicated foci has been reported and appears to vary with growth conditions (Sunako et al., 2001; Bates and Kleckner, 2005; Nielsen et al., 2006a; Adachi et al., 2008; Espéli et al., 2008). This process seems to be more persistent for loci located near the terminus of replication (Li et al., 2003; Bates and Kleckner, 2005; Espéli et al., 2008). The loss of colocalization occurs simultaneously at various positions on the chromosome when much of the chromosome is replicated (Bates and Kleckner, 2005; Espéli et al., 2008).

The mechanisms responsible for structuring the chromosome in MDs are largely unknown. A likely model postulates that internal organization of the different MDs involves recognition of a domain-specific repeated motif by a protein that would isolate

this domain from the others. Such an organization would be reminiscent of two systems characterized in the Ori-proximal region of the *Bacillus subtilis* chromosome, the Spo0J-*parS* and the RacA-*ram* systems. Spo0J interacts with eight to ten *parS* sites scattered over a region of 600 kb (Lin and Grossman, 1998), whereas 25 copies of a 14 bp *ram* sequence scattered over the 612 kb Ori region are bound by RacA (Ben-Yehuda et al., 2005). Here, we report use of a statistical analysis to predict an "MD signature" motif, i.e., a motif specifically enriched in one MD that could be the target of such a protein. We report the identification of the landmark signature sequence of the Ter MD, a 13 bp motif called *matS*, repeated 23 times in the 800-kb-long region. We identify the protein MatP that interacts in vivo with the motif *matS*. We further demonstrate that the *matS*-MatP-specific interaction is crucial for Ter MD organization. In the absence of MatP, segregation of the Ter MD occurs early in the cell cycle, and markers in the Ter MD exhibit mobility similar to that of markers in NS regions. Mutational analysis of *cis*-acting *matS* sites provides information on the mechanism used by MatP to compact DNA over a large distance. On the basis of these observations, we propose a model for spatial organization of the Ter MD by MatP during the cell cycle.

RESULTS

matS Is the Signature Motif of the Ter Macrodomain

We hypothesized that scattered DNA binding sites for an architectural protein are likely candidates as MD organization determinants of the *E. coli* chromosome. To predict hypothetical "domain signature" motifs, we used a statistical approach, as described before (Halpern et al., 2007). It consisted of evaluating the exceptionality of all motifs of a given length inside an MD (exceptionality score) and comparing it to their exceptionality outside the domain (contrast score, i.e., the p value of a binomial test). Exceptionality was evaluated by comparison of observed to expected counts of each word of a given length, with the mono- to hexanucleotide composition of the Ter domain being taken into account. The analysis focused on 11-nt-long words, because in a learning case based on detection of the *parS* motif in the Origin proximal domain of the *B. subtilis* genome, this length proved relevant for detection of one of the *parS* subsequences as the most highly exceptional (Experimental Procedures and the Supplemental Experimental Procedures available online). Exceptionality of each of the 505,775 11-mers present in the Ter MD is plotted as a function of its contrast score in Figure 1A. Among the most exceptional and contrasted words, six were overlapping (Figure 1A, and Table S1); they allowed the identification of a 13-mer consensus sequence presented on Figure 1B. When the 13-mer GTGACRNYGTCAC sequence was searched on the whole *E. coli* genome, it was found 21 times between coordinates 1135 kb and 1900 kb (Figure 1C and Table S2), which approximates the extent of the Ter MD (1220 kb to 1900 kb [Espéli et al., 2008]). This motif therefore appeared to be a good candidate for organizing the Ter MD; we called it *matS* for *ma*crodomain *T*er sequence. Allowing one nucleotide difference in the *matS* consensus sequence revealed the presence of only four additional sites in the entire chromosome, two located in the Ter MD (*matS5* and *matS17*) and two in the Left MD (pseudo-*matS*

L1 and L2). The *matS* motif was also found as a repeated motif in the genome of γ-proteobacteria, in Enterobacteriaceae and in Vibrionaceae species. Moreover, the concentration of *matS* sites in the region opposite the replication origin was conserved in these species (Figure 1D).

matS Is Specifically Bound by MatP

Electromobility shift assays (EMSAs) performed with crude *E. coli* extracts revealed the specific binding of a factor to *matS* (data not shown). To identify the gene encoding this factor, we took advantage of a streptomycin selection system that allows identification of genes encoding DNA binding activity. In brief, expression of a gene conferring streptomycin sensitivity may be modulated by the binding of a protein to its target sequence (e.g., *matS*) located in the promoter region. Using a multicopy genomic library, we were able to select transformants that displayed reduced streptomycin sensitivity (i.e., candidates to bind *matS*). We identified seven clones containing the same genomic region extending from *ycbZ* and *ompA*. The only complete open reading frame (ORF) found in every clone was *ycbG* (renamed *matP* for *ma*crodomain *Ter p*rotein). *matP* encodes a 17 kD unknown protein conserved in Enterobacteriaceae and Vibrionaceae species and to a lesser extent in Pasteurellaceae species. Structure predictions revealed a ribbon-helix-helix domain observed in a number of transcription factors and plasmid partition systems and a coiled-coil C-terminal domain. Interestingly, MatP belongs to a group of proteins (including SeqA and MukBEF) that are exclusively identified in bacteria carrying Dam methyltransferase activity (Brezellec et al., 2006).

Using a two-step purification procedure, we purified MatP to near homogeneity. MatP was soluble and formed dimers in solution (data not shown). Using EMSA, we confirmed specific binding of MatP to *matS* (Figure 2A); the K_d of the MatP dimer for a double stranded 41 bp oligonucleotide containing *matS* was about 8 nM (Figure 2B). Competition assays revealed that MatP binds *matS* more than 100 times more efficiently than the degenerate sites present in the Left MD (Figure S1).

The in vivo DNA binding pattern of MatP was analyzed by formaldehyde-mediated protein crosslinking followed by immunoprecipitation of MatP-containing complexes with anti-MatP antibodies (chromatin immunoprecipitation [ChIP] assay). DNA recovered from the ChIP fraction was analyzed by polymerase chain reaction (PCR) with various pairs of primers. Results presented in Figure 2C indicated that *matS* sites were specifically enriched; PCR fragments corresponding to five *matS* sites were detected, whereas three control fragments devoid of the *matS* site were not amplified. A similar analysis was performed in a strain in which *matS22* and *matS23* had been deleted (Figure 2D). No fragments corresponding to *matS22* and *matS23* regions could be amplified in the ChIP fraction, whereas fragments overlapping *matS18*, *matS19*, and *matS20* were amplified. These results showed that MatP binding to a fragment in vivo was dependent on the presence of a *matS* site. The binding pattern of MatP in the *matS23* region in a WT strain was analyzed in more detail. Several primer pairs amplifying fragments located at various distances from *matS23* were used (Figure 2E). No amplification was revealed for fragments located at a distance of 5 kb or 10 kb from the *matS* site, indicating that MatP does not spread from *matS23* far into flanking DNA.
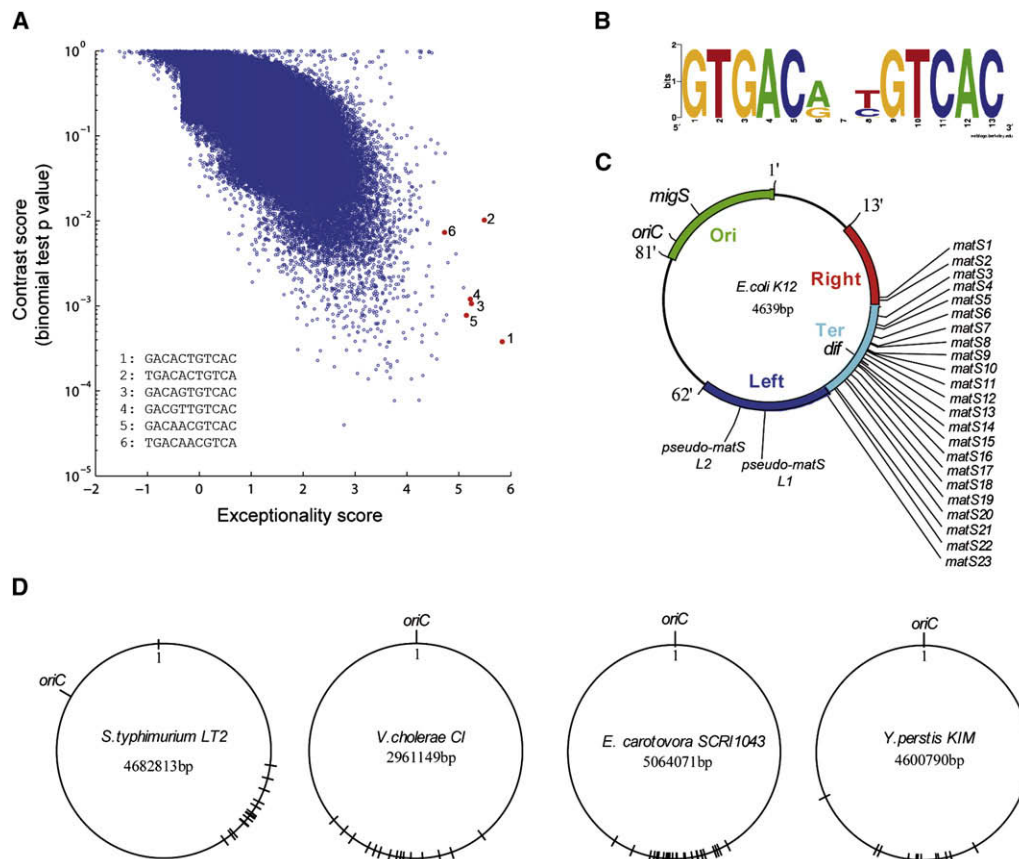
Figure 1. *matS* Sites Are Clustered in the Ter Macrodomain of the *E. coli* Chromosome

(A) Each 11-mer was plotted according to its exceptionality in the Ter MD (abscissa axis) and to the contrast bias between the Ter MD and the rest of the chromosome (ordinate axis). The 505,775 11-mers found in the Ter domain are indicated by blue circles. The six overlapping words are indicated in red together with the nucleotide sequence.

(B) A Logo 13 bp consensus palindromic sequence deduced from 21 *matS* motifs (see main text) has been defined with the Weblogo program (http://weblogo. berkeley.edu/).

(C) Distribution of 21 *matS* sites and four *matS*-like sites in the *E. coli* chromosome. Twenty-one motifs were found between coordinates 1135 kb and 1900 kb. Four sites differing by 1 nt change are present in the chromosome, two located in the Ter MD (*matS5* and *matS17*), and two in the Left MD (pseudo-*matS* L1 and L2). Colored bars represent the different MDs (coordinates are indicated in minutes).

(D) The localization bias of *matS* sites is conserved among enterobacteria, *Vibrio*, and *Pasteurella* species. Distribution of repeated *matS* sites in a 600–1000 kb large region opposite to *oriC* in the chromosome of *Salmonella typhimurium* LT2, *Erwinia carotovora* subsp. *atroseptica*, *Vibrio cholerae* (chromosome I), and *Yersinia pestis* KIM.

To map the binding sites for MatP on a genome-wide basis, we used DNA from the ChIP fraction as a probe to hybridize macroarrays that contain the complete set of open reading frames (ORFs) in the *E. coli* genome. The amount of specific MatP binding or enrichment factor was estimated by subtraction of the normalized abundance of a locus in the ChIP fraction of a *matP* strain to the abundance of the same locus in the ChIP fraction of the WT strain and by division of this value by its normalized abundance in total DNA. The relative enrichment factor was plotted versus genome position (Figure 2F). These results revealed a limited number of ORFs bound by MatP (Table S8). Strikingly, among the most enriched 30 ORFs, 25 contained or were adjacent to a *matS* sequence, indicating that *matS* sequences constitute the main targets of MatP on the chromosome (Figure 2G). Furthermore, it showed on the genome scale that MatP does not

spread far into DNA flanking *matS* sites since ORFs separated from *matS* sites by a few kb were not enriched.

matP Inactivation Causes Severe Defects in Chromosome Segregation and Cell Division

In exponential phase in rich medium (doubling time, $\tau = 30$ min), deletion of *matP* induced severe chromosome segregation and cell-division defects (Figures 3A and 3B): a significant number of cells were anucleate (7%), whereas small and long filamentous cells displayed condensed nucleoids (12%). It is noteworthy that the amount of filamentous and anucleate cells was maximal in exponential phase and decreased as cells entered stationary phase. Cell filamentation is often associated with the activation of a DNA repair pathway, called SOS induction. *matP* cells remained viable in rich medium when SOS induction was prevented by
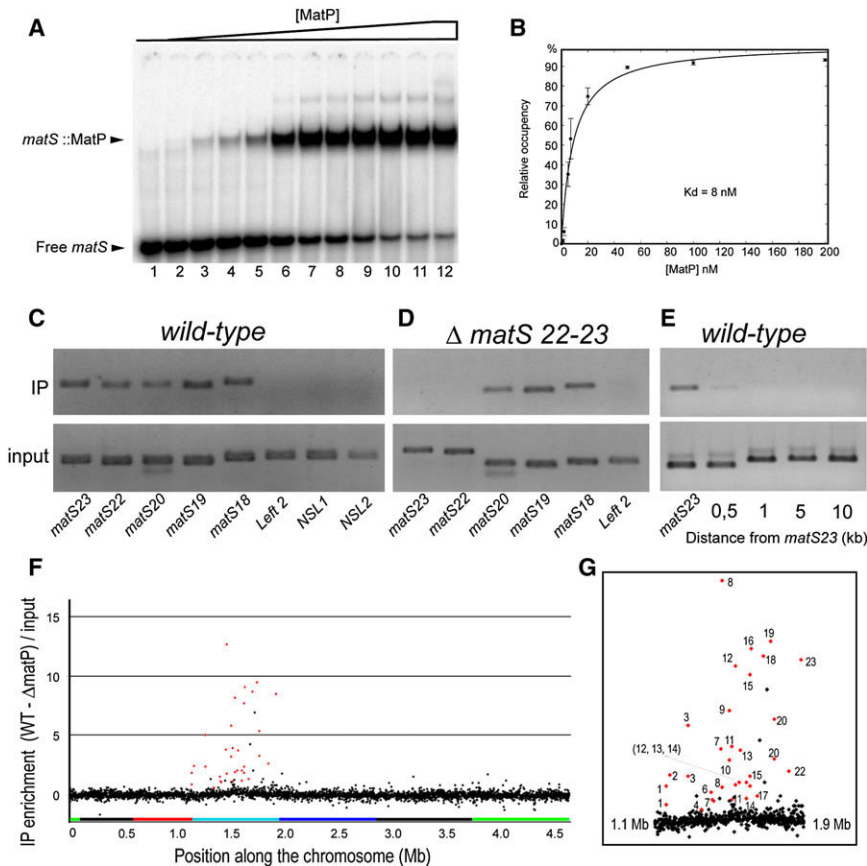
Figure 2. Specific Interaction of MatP with *matS* Sites

(A) EMSA of a double-stranded oligonucleotide containing *matS19* was performed with increasing concentrations of MatP in the presence of 24 μM nonspecific competitor DNA. MatP concentrations were 0 nM (lane 1), 0.1 nM (lane 2), 0.5 nM (lane 3), 1 nM (lane 4), 2 nM (lane 5), 5 nM (lane 6), 7 nM (lane 7), 10 nM (lane 8), 20 nM (lane 9), 50 nM (lane 10), 100 nM (lane 11), and 200 nM (lane 12).

(B) The occupancy of the *matS* site was plotted as a function of MatP concentration. The binding data were fit to a simple binding isotherm as described before (Murtin et al., 1998).

(C) Chromatin immunoprecipitation assay of MatP on the *E. coli* chromosome. An affinity purified αMatP polyclonal antibody was used to immunoprecipitate regions of the chromosome crosslinked to MatP (ChIP fraction). PCR probes were designed to detect 300 pb fragments containing various *matS* sites or chromosomal regions without *matS* sites (NSL1, NSL2, and Left 2).

(D) Chromatin immunoprecipitation assay of MatP on the chromosome of a strain where *matS22* and *matS23* were deleted.

(E) In vivo MatP spreading from *matS* sites was tested by ChIP with probes located 0.5, 1, 5 and 10 kb away from *matS23*.

(F) ChIP-on-chip assay for MatP binding. Panorama gene arrays (Sigma-Genosys Biotechnologies) carrying the 4287 *E. coli* ORFs were hybridized with labeled DNA from the ChIP fraction obtained from a WT strain, with labeled DNA from the ChIP fraction of a *matP* strain, and with total DNA of a WT strain, and quantified (see main text). ORFs with results above the background and containing or flanking *matS* sites are labeled in red. Colored bars represent the different MDs as indicated in Figure 1.

(G) Zoom of the Ter MD region. ORFs containing or flanking *matS* sites were indicated according to their number on Figure 1C. Only *matS5* and *matS21* were absent among the 30 most MatP-enriched ORFs.

a *recA* mutation; furthermore, no SOS induction was detected in *matP* cells (data not shown), indicating a lack of chromosomal damage. In contrast, in minimal medium (τ = 70 min), most cells displayed a WT phenotype at every step of the growth curve (Figure 3B, and see below). The average number of origins per cell was predicted from the number of chromosomes measured by cytometry after the addition of rifampicin, which prevents reinitiation of chromosome replication (rifampicin run-out experiments). This number of origin was similar in both WT and *matP* cells; it was estimated around six (not considering filamentous cells) in rich medium and three in minimal medium, indicating that initiation of replication in both strains occurs halfway through the cell cycle in both conditions (Figure S2). The duration of the replication (C period) was estimated directly on the microscope slide by measurement of the fraction of the cell cycle when replisomes were functional, as revealed by the detection of SSB-YFP foci (Reyes-Lamothe et al., 2008). A modest decrease in the number of cells without SSB foci was observed in the *matP* strain and can be interpreted as a longer C period, 86 min and 94 min in the WT and the *matP* strains, respectively (Figure S3). Altogether, these results indicated that *matP* inactivation affected chromosome segregation in rich medium but without inducing significant DNA damage or changes in replication regulation.

Long-Range DNA Interactions between the Right and the Ter MDs Are Affected by MatP Inactivation

Long-distance DNA collisions revealed by the frequency of site-specific recombination between λ *att*L and *att*R loci inserted at different chromosome locations can be used to reveal chromosome conformation (Valens et al., 2004). These interactions have been measured in WT and *matP* cells grown in minimal medium (Figure 3C). As observed before, interactions between *att*R inserted in the Right MD and *att*L sites inserted in the Ter MD were low in WT cells because they belong to different MDs. Remarkably, the collisions were more frequent in *matP* cells. In contrast, interactions within the Right MD or between the Right MD and other regions of the chromosome were comparable in WT and *matP* cells. These results indicate that in *matP* cells, Right MD DNA collides with a higher probability with the flanking Ter MD, suggesting a disorganization of Ter MD.

MatP Colocalizes with the Ter Macrodomain throughout the Cell Cycle

To determine the cellular position of MatP, we constructed a strain containing a chromosomally encoded version of *gfp* fused to *matP* under the control of the *matP* promoter. In rich medium,
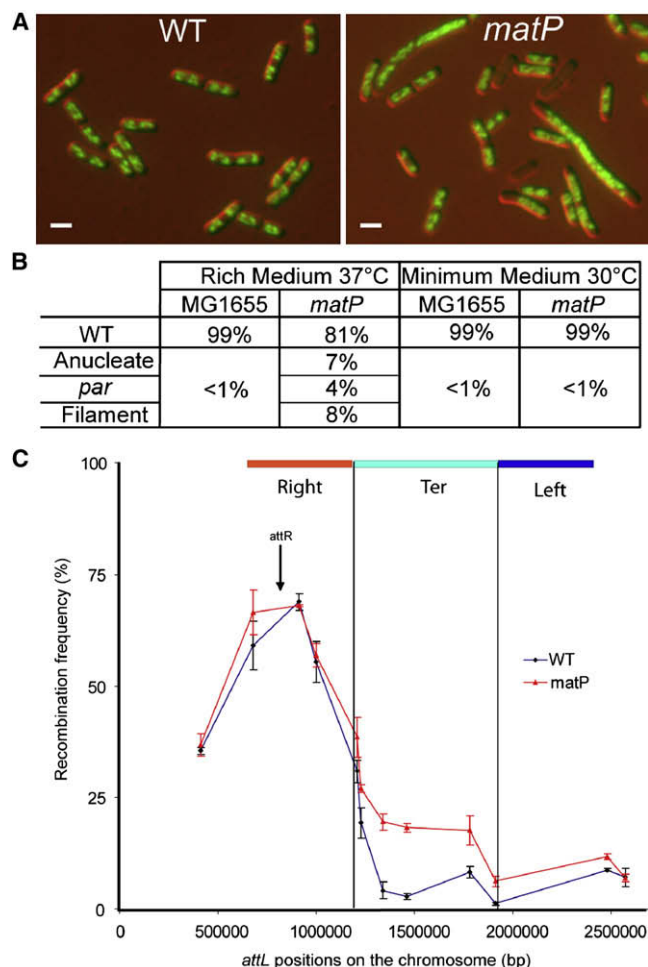
Figure 3. Cell Division and Chromosome Segregation Defects in *matP* Cells

(A) Representative cells of *E. coli* MG1655 and the *matP* isogenic derivative grown in exponential phase (OD_{600} 0.4) in Lennox Rich Medium at 37°C. Nucleoids were stained with DAPI (green).

(B) Quantification of the different types of cells observed in rich and minimal medium. "*par*" indicates cells with mispositioned condensed nucleoids. "Filaments" indicates the presence of filamentous cells.

(C) Long-distance DNA interactions revealed by λ Int recombination assay. The recombination frequency between *att*R located at 17′ (indicated by an arrow) in the Right MD and various *att*L sites in the NS region, the Right, Left, and Ter MDs (Table S6) was measured upon induction of the Xis and Int recombinases in WT (blue) and *matP* (red) cells. The Right, Ter, and Left MDs are indicated by colored lines above the graph.

this strain displayed no filamentous or anucleate cells, indicating that the MatP-GFP fusion protein was functional. We followed throughout the cell cycle the subcellular localization of MatP by time-lapse live microscopy (in minimal medium at 25°C; τ = 120 min). MatP formed discrete foci, indicating that MatP accumulated at specific locations in the cell. In newborn cells, MatP foci localized near the new pole. As cells progressed in the cell cycle, the MatP focus migrated to the midcell, where it remained for a period as long as 60 min. Finally, about 30 min before division, the MatP focus split, and the two sister foci remained

juxtaposed for a few minutes before moving away from midcell (Figures 4A and 4B, Movie S1). This localization pattern was also observed at a faster growth rate in a snapshot analysis (τ = 70 min at 30°C; Figures S4A and S4B) and at a slower growth rate (τ = 120 min at 30°C; Figure S4D).

The localization pattern of MatP-GFP was remarkably similar to that observed for chromosomal markers in the Ter MD (Li et al., 2003; Bates and Kleckner, 2005; Espéli et al., 2008). Therefore, we analyzed the colocalization of a focus generated by a fusion of *matP* to the gene encoding mCherry with two foci corresponding to chromosomal markers revealed by two different *parS*/ParB systems (Nielsen et al., 2006b). We used two markers inserted 100 kb apart in the Ter MD (Figure S5), two markers inserted 350 kb apart in the Ter MD, or two markers inserted outside the Ter MD 1270 kb apart in Right and Left MDs (Figures 4C–4F, Figure S5). Chromosomal markers located 100 kb or 350 kb apart in the Ter MD colocalized with or contacted the MatP focus in 85% of the cells. Colocalization of the MatP focus with a Ter locus was also observed with the *lacO*-LacI fluorescent repressor operator system (FROS) (data not shown). Contrasting results were obtained with chromosomal markers inserted outside the Ter MD: the MatP focus was rarely (<5%) colocalized with both chromosomal markers (Figures 4D and 4F).

Interaction of MatP with *matS* Prevents Early Segregation of Duplicated Ter Macrodomains

After replication, the length of the colocalization period of sister chromosomal loci changes according to their belonging to MDs or NS regions. These differences result in abrupt changes in the proportions of cells with 1, 2, or 4 foci at the boundaries of the Right, Ter and Left MDs (Figures 5A and 5B) (Espéli et al., 2008). In *matP* cells, we observed a dramatic decrease in the proportion of cells with one focus for markers located in the Ter MD. Whereas more than 80% of the WT cells presented only one focus for most markers in the Ter MD, this number was reduced to about 50% in *matP* cells (Figures 5A and 5B). Similar results were obtained with the *lacO*-LacI FROS system (Figure S6). Since the proportions were unchanged in other MDs and NS regions, we conclude that MatP inactivation specifically affected the Ter MD. Because MatP inactivation did not alter the cell-cycle parameters in minimal medium (see above), these results suggested that MatP inactivation specifically affected the colocalization step between the duplicated Ter MDs.

The effect of MatP inactivation on Ter MD segregation was directly visualized with live microscopy. Time-lapse experiments with 1 min intervals were performed for analysis of the position of a marker in the Ter MD (Ter-6 at position 1689 kb) over a period longer than 120 min, i.e., the duration of a complete cell cycle in these conditions (Figure 5C, see above). In WT cells (Figure 5D), the focus moved from the pole in the newborn cell to midcell and then split into two sister foci 30 min before division. This segregation drove the focus to a very precise final position at midcell, the home position, as visualized by the remarkably small standard deviation (between 60 and 80 min after birth) (Figure 5D and Movie S2). Strikingly, the segregation pattern of Ter-6 marker was radically different in *matP* cells for three parameters (Figure 5E, Movie S3). First, a transient individualization step where sister foci fuse and separate several times was observed
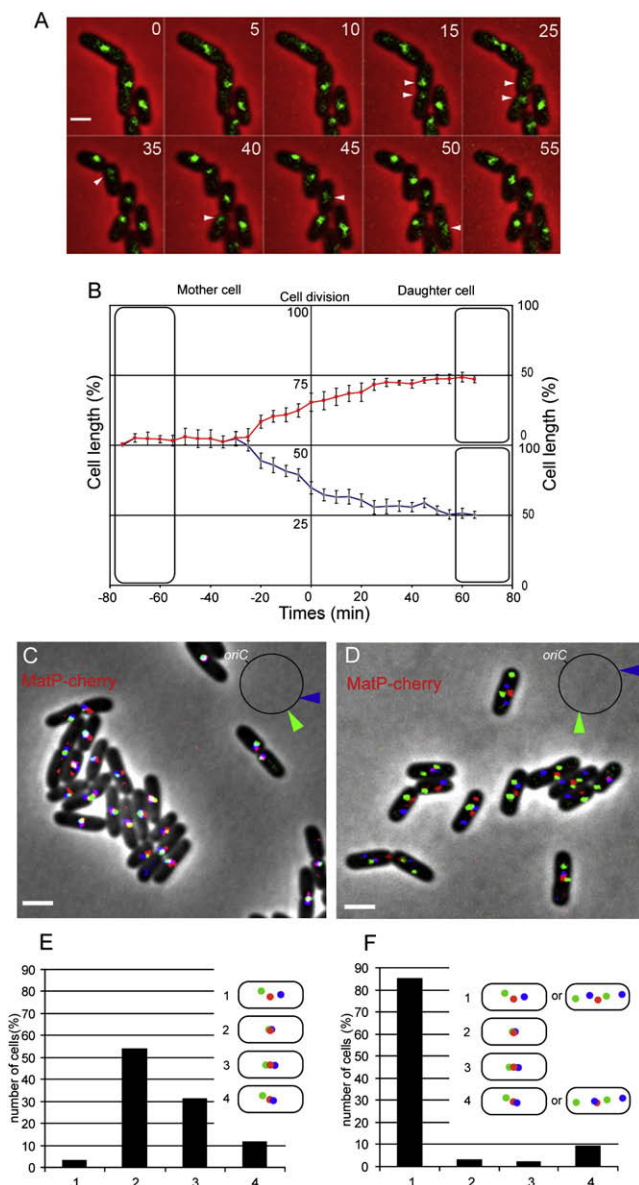
Figure 4. MatP-GFP Foci Colocalize with Markers of the Ter Macro-domain

(A) Dynamics of MatP-GFP foci observed by live microscopy during the cell cycle. A picture was taken every 5 min over a period of 60 min (τ = 120 min; see main text). MatP-GFP is not evenly distributed but appears as foci. The scale bar represents 2 μm.

(B) Segregation pattern of Mat-GFP foci during the cell cycle obtained from the average of 15 cells. The position of the foci along the long axis of the cell is expressed as a percentage of the cell length. Mother and daughter cells are represented on the left and right of the panel, respectively.

(C) Colocalization of the MatP-mCherry focus (red) with two *parS* markers, localized 350 kb apart in the Ter MD, labeled with ParB[T1]-YFP (blue) and ParB[P1]-CFP (green). The scale bar represents 2 μm.

(D) Colocalization of the MatP-mCherry with two *parS* markers localized 1270 kb apart in the Right MD marked with ParB[T1]-YFP (blue) and in the Left MD marked with ParB[P1]-CFP (green). The scale bar represents 2 μm.

(E and F) Quantification of the colocalization of the MatP-mCherry focus with the chromosomal markers obtained in (C) and (D), respectively. The different types of cells are indicated in each panel. Two hundred cells were analyzed.

over a long period, from 20 to 50 min after birth. Second, final separation of sister foci occurred early in the cycle, 70 min before division compared to 30 min in WT cells. This early segregation of Ter MDs in *matP* cells accounted for the reduced number of cells with one focus for markers in the Ter MD (Figure 5B). Third, the focus was localized less precisely at the home position in the *matP* cells than in WT cells. Altogether, these results showed that the inactivation of MatP resulted in early segregation of Ter markers.

The three external *matS* sites located at the border with the Left MD (*matS21-23*) were deleted and the proportion of cells with one, two, three, or four foci in strains carrying chromosomal markers located at four different positions in the Ter MD (Ter-6, Ter-7, Ter-8) or in the Left MD (Left-3) were analyzed in snapshot experiments (Figure 5F). The deletion of the three *matS* sites decreased the number of cells with one focus from 66% to 46% for the Ter-8 marker. This effect was as profound as the inactivation of MatP. The distribution was unchanged concerning markers Ter-6 or Left-3 that are distant from deleted *matS* sites. Altogether, these results showed that the absence of interaction of MatP with *matS* sites specifically affected the region of the Ter MD adjacent to the considered *matS* sites and induced early segregation of its markers.

Ter Macrodomain Organization Is Mediated by MatP

The local effect of *matS* site deletions was examined in greater detail. Whereas the deletion of the three *matS* sites bordering the Ter MD (*matS21-23*) affected the number of foci of the border marker Ter-8 as much as MatP inactivation, their deletion had only a partial effect on the marker Ter-7 (Figure 5F). This suggested that *matS20* may still influence the foci copy number of Ter-7, located 40 kb away. Similarly, deletion of only *matS23*, or both *matS22* and *matS23*, only slightly affected the number of Ter-8 foci, indicating that *matS21* influences Ter-8, a locus located 50 kb away. This effect seems to be lost, however, at a distance of 150 kb because *matS20* has no apparent effect on Ter-8. These results fit with the density of *matS* sites in the Ter MD, which is on average one site every 40 kb, and indicate that the MatP-mediated organization of Ter MD affects DNA colocalization over a large distance.

To determine whether the effect of MatP on foci colocalization was associated with compaction, we measured the interfocal distance between different markers in WT and *matP* strains. In *matP* cells, the average interfocal distance between two markers 100 kb distant in the Ter MD was increased by 2-fold compared to WT cells (0.27 μm versus 0.15 μm; Figures 6A–6C). A comparable increase in interfocal distance was also observed upon inactivation of MatP for markers 350 kb distant in the Ter MD (data not shown). These results indicate that MatP influences DNA compaction.

Constraints on mobility are apparent in MDs, whereas in NS regions, DNA markers exhibited a greater mobility (Espéli et al., 2008). To assess the influence of MatP on DNA mobility, we measured the total distance traveled by loci from the Ter MD in WT and in *matP* cells over a 5 min period (Figure 6D). In *matP* cells, the Ter-6 and Ter-8 loci traveled a distance about four times greater than that crossed by the same loci in WT cells (1.2 μm versus 0.3 μm). These loci became as mobile as loci in the NS regions. The diffusion coefficient of these loci can be
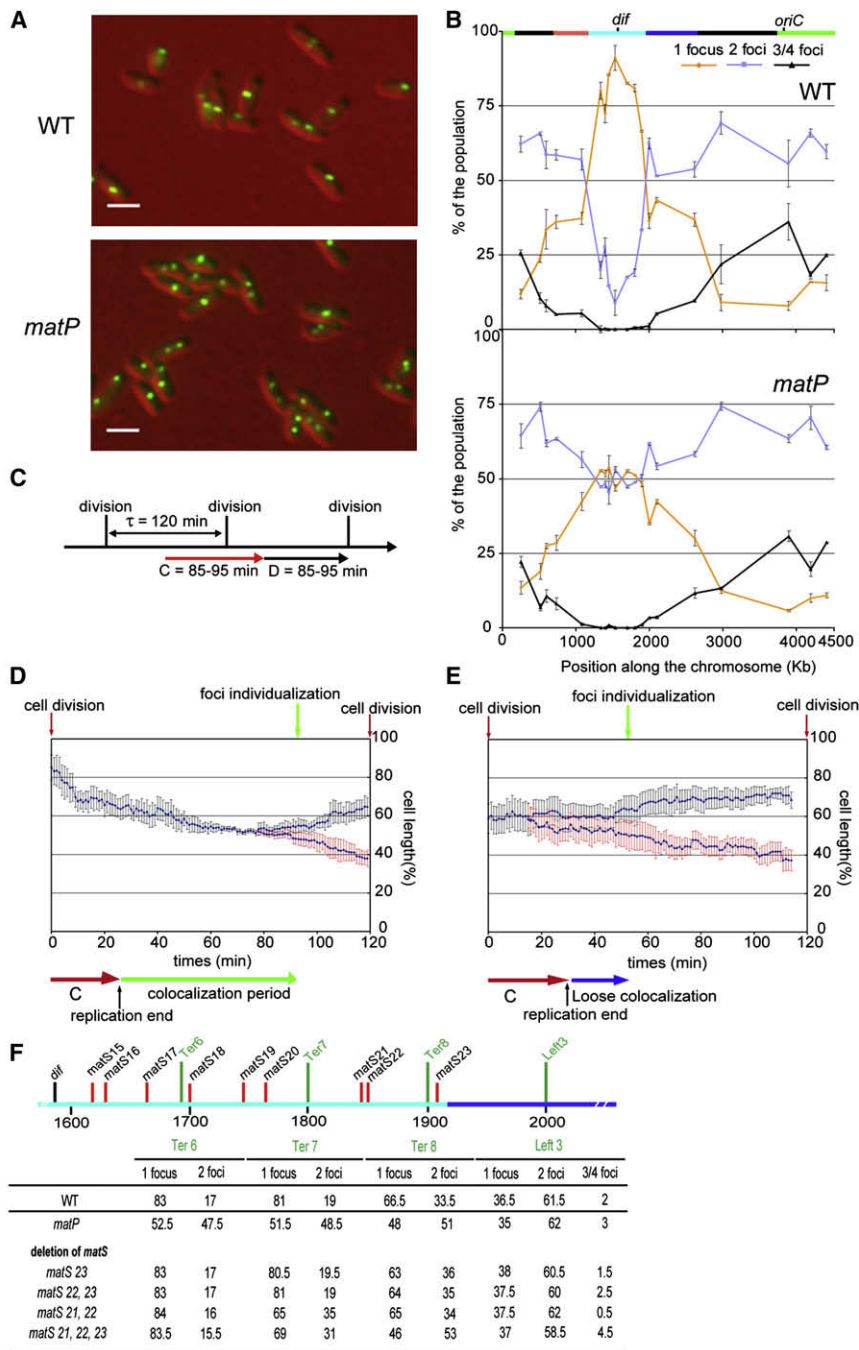
Figure 5. MatP Modulates the Colocalization Step of the Ter Macrodomain

(A) Distribution of the Ter-6 *parS* marker labeled with ParB[P1]-GFP in WT and *matP* cells. Scale bars represent 2 μm.

(B) Quantification of the number of foci observed per cell for 19 markers in WT (top) and *matP* (bottom) cells (position of markers is indicated in Figure S7 and Table S5). An MD map is drawn at the top of the graph. About 300 cells were counted for each locus. Striking changes are only observed in the Ter MD.

(C) Schematic representation of the cell-cycle parameters observed for the time-lapse experiment conditions at 25°C in minimal medium A. D period corresponds to the time between the end of replication and division.

(D) Averaged segregation pattern of the Ter-6 marker in WT cells observed during time-lapse experiments. The localization of foci in 20 cells was averaged after synchronization according to the division time. The position of the foci along the long axis of the cell (indicated by the percentage of the cell length) was plotted over time. The end of the replication C period, the period of foci colocalization, and the time of foci individualization are indicated.

(E) Averaged segregation patterns of the Ter-6 marker in a *matP* strain as in (D). The loose colocalization period corresponds to the time interval during which individualized foci collide with each other several times without any precise segregation direction.

(F) Effect of *matS* sites on the number of foci observed per cell for four markers located in the Ter and Left MDs. Genetic map of the Ter-Left MD border region is shown. Positions of the *parS* tags and the *matS* sites are indicated. The proportion of observed cells with one, two, or three to four foci of the Ter-6, Ter-7, Ter-8, and Left-1 markers, as measured in (B), is reported in different strains carrying deletion of specific *matS* sites.

DISCUSSION

Chromosome Organization and the Ter Macrodomain

Understanding of chromosome architecture and dynamics remains fragmentary in both prokaryotic and eukaryotic cells. By measuring the relative probabilities of collisions between different pairs of loci scattered over the *E. coli* genome and by tracking fluorescent reporters, we have shown that the chromosome is organized in MDs and less constrained NS regions and that the behavior of loci belonging to the MDs and to the NS regions is radically different (Valens et al., 2004; Espéli et al., 2008). Among the different mechanisms that may account for this chromosome structuring, we have now provided evidence that a site-specific system, composed of the DNA binding protein MatP and its target *matS* sites, organizes the 800-kb-long chromosomal Ter MD.
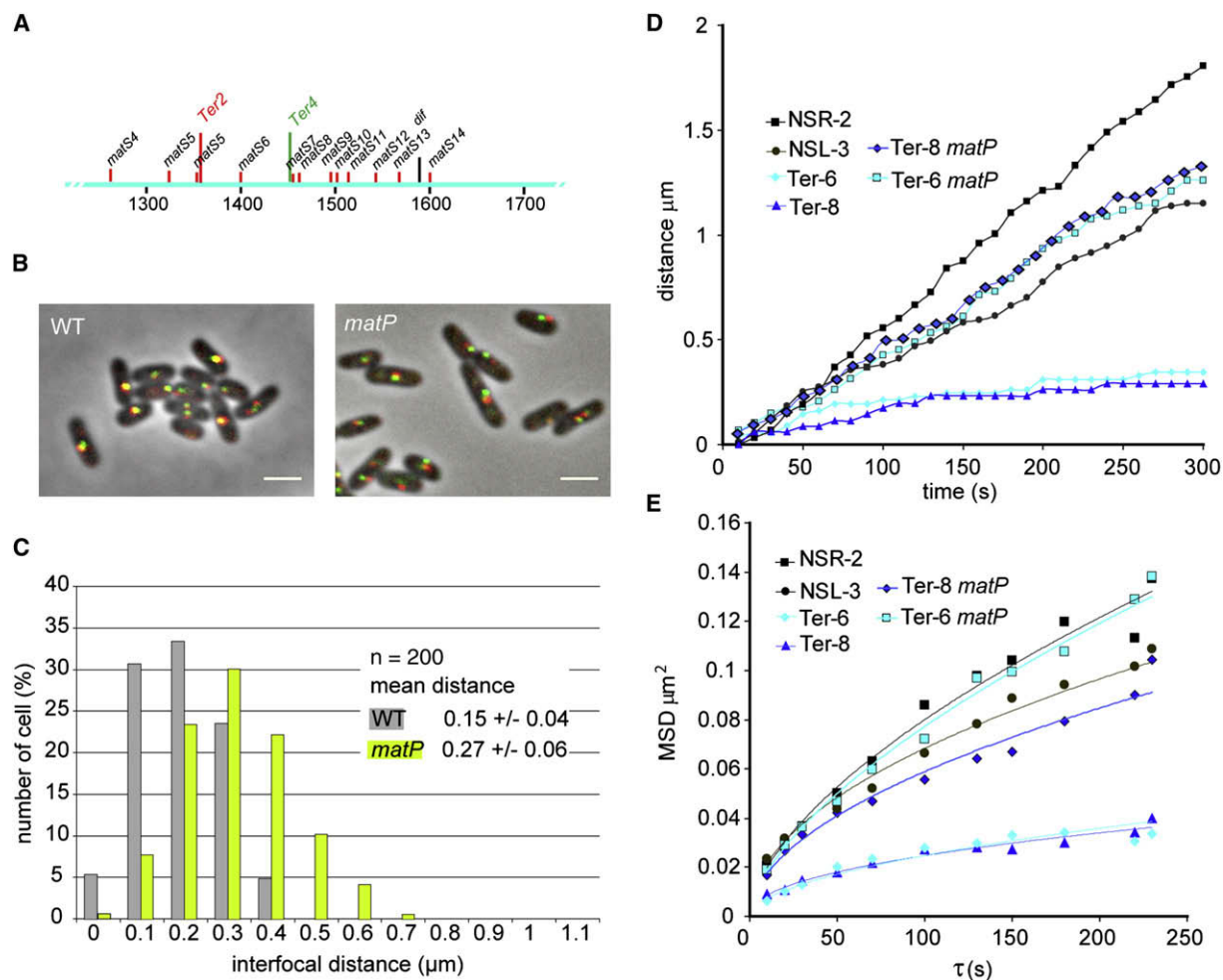
approximated from the mean square displacement (Figure 6E) as described before (Espéli et al., 2008). At home position, each locus presents a subdiffusive mode of movement. In *matP* cells, the diffusion coefficient of both Ter-6 and Ter-8 loci was two to four times greater than that in the WT strain ($D_{\tau 1-2} \sim 3.5 \times 10^{-12} cm^2/s$ versus $D_{\tau 1-2} \sim 1.5 \times 10^{-12} cm^2/s$), indicating that these markers occupy a cage two to four times larger in *matP* cells than in WT cells (i.e., ~400 nm × 400 nm compared to ~200 nm × 200 nm).

Figure 6. MatP Controls DNA Compaction and Constrains DNA Mobility in Ter Macrodomain

(A) Genetic map of the *matS*4-*matS*14 segment of the Ter MD with coordinates indicated in kb. Position of the Ter-2 and Ter-4 *parS* markers, of *matS*4-*matS*14 sites and of the *dif* site is indicated.

(B) Interfocal distance was measured between foci of two Ter MD markers in WT and *matP* cells. Scale bars represent 2 μm.

(C) Histogram representing the proportion of cells with the different interfocal distances in WT and *matP* cells.

(D) The mobility of various loci in the chromosome was estimated by measurement of the absolute movement of the foci at the home position in time-lapse experiments with 10 s intervals (NSR-2, NSL-3, Ter-6, Ter-8 [indicated in Figure S7]). The x-y coordinates of the foci at every time point were recorded, and the distances traveled in the 10 s interval were calculated. The absolute value of the distance for every interval was added progressively over 5 min. The mobility of Ter-6 and Ter-8 markers was measured in both WT and *matP* cells and that of NSR-2 and NSL-3 in WT cells.

(E) Mean square displacement (MSD$_{xy}$) for time intervals (τ) between 10 and 250 s are plotted on linear axes for the markers indicated in (D).

The existence of the Ter MD was questioned in a study that reported independent spatial positioning and an asymmetric pattern of segregation of two markers located at 150 kb from each other in the Ter MD (Wang et al., 2005). Data reported here support the existence of a Ter MD. First, our data indicate that belonging to the Ter MD does not imply permanent spatial and temporal colocalization since in 35% of the cells, foci of markers separated by 350 kb within the Ter MD can contact the MatP focus without overlap, while the three foci overlapped in only 50% of cells. Second, we did not find any evidence for splitting of the Ter MD since MatP-GFP foci segregate symmetrically as one entity in WT MG1655 cells devoid of any FROS system that might perturb Ter MD segregation. Colocalization of reporters from different

FROS systems with the MatP focus is consistent with the symmetric segregation pattern of Ter loci reported in several studies with FISH or FROS (Niki et al., 2000; Li et al., 2003; Bates and Kleckner, 2005; Adachi et al., 2008; Espéli et al., 2008). Discrepancies could originate from the strain and growth conditions used by Wang et al. (2005): both the number and the position of MatP foci in strain AB1157 grown in minimal medium with glycerol differ from those found either for strain MG1655 grown in the same conditions or for the same AB1157 strain grown at a faster rate (Figure S4).

Organization of the Ter MD by MatP
By interacting with multiple dispersed target sites over a large region of the chromosome, MatP is reminiscent of the Spo0J and

RacA systems. Chromosome segregation upon entry into sporulation in *B. subtilis* involves remodeling and anchoring of the chromosomes to the cell poles. RacA binds preferentially to *ram* sites but also with less affinity to the bulk chromosomal DNA. Strong protein-protein interactions allow DNA compaction. RacA molecules bound to *ram* sites form an adhesive structure that anchors the origin regions at the poles, while nonspecific binding of RacA to the entire chromosome may induce remodeling of the chromosome into a serpentine-like nucleoid (Ben-Yehuda et al., 2005). Spo0J, upon binding to *parS* sequences, spreads into flanking DNA over 5–10 kb, forming "Spo0J domains" (Murray et al., 2006). The long-range organization of the *oriC* region is modulated by Soj protein that has the ability to coalesce different Spo0J domains (Marston and Errington, 1999). The role of Spo0J spreading in the Ori region is not clearly defined and may be required for the proper positioning and/or the organization of the *oriC* region. The comparison between MatP and RacA or Spo0J may be limited to the distribution of the target sequences because both the mechanisms used and the rationale for organizing chromosomal subregions are different. Concerning the mode of interaction with DNA, MatP binds *matS* sequences, and no spreading to flanking DNA or nonspecific binding to other regions has been detected. On average, *matS* motifs are present at one copy every 40 kb, and *matS* sites exert effects over distances greater than 40 kb (Figure 5). Different mechanisms can be proposed to explain how MatP dimers interact with and affect DNA over a large distance. First, one can imagine that the relative proximity of several *matS* sites in supercoiled plectonemic DNA allows contacts between the different dimers of MatP bound to *matS* sites and that the intervening DNA would be looped out. Such a mechanism would be reminiscent of the functional filament aggregates formed by the polymerization of SeqA dimers (Guarne et al., 2005). In an alternative model, *matS*-MatP complexes might act as nucleation sites for an as-yet-unknown factor that does spread several kb along the DNA.

MatP also contrasts with Spo0J and RacA by organizing the region opposite to *oriC* rather than the Ori region itself. MatP appears to be the first protein described that is involved in the organization of the chromosome terminus. It is not yet known whether MatP localization relies on the interaction with a particular cellular structure as observed for RacA or whether it depends on the orientation of the chromosome and the position of *matS* sites in the cell as observed for Spo0J (Lee et al., 2003). The MatP focus is present and shows dynamic behavior during the entire cell cycle, suggesting that attachment to the chromosome rather than anchoring to a cellular structure might account for the localization of MatP foci.

Control of Ter MD Segregation by MatP
Segregation of the *E. coli* chromosome has been described in different studies. Several studies agree on the existence of an extended colocalization of duplicated Ter regions that segregate only a few minutes before division (Li et al., 2003; Bates and Kleckner, 2005; Adachi et al., 2008; Espéli et al., 2008). A striking defect associated with MatP inactivation is the early segregation of duplicated Ter MDs (Figure 7). Remarkably, MatP inactivation is specific for Ter MD segregation since the segregation of markers in other regions is not affected. Our results confirm
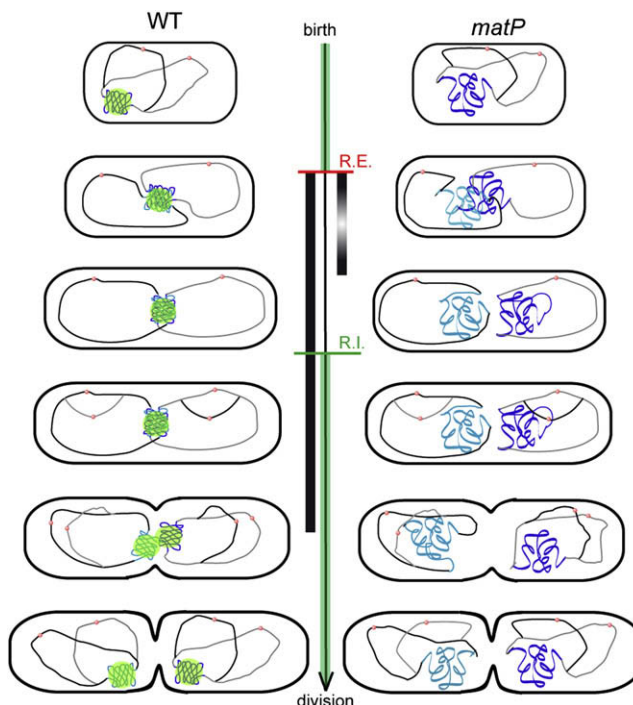

Figure 7. A Model for MatP-Dependent Ter Macrodomain Organization during the Cell Cycle
The organization of the Ter MD (blue/cyan lines) by MatP is represented through selected steps of the cell cycle in WT (left) and *matP* (right) cells. In the WT strain, the MatP focus is represented as a green disk that coincides with the Ter MD territory. In WT cells, the colocalization of the condensed Ter MDs remains until 30 min before division (vertical black bar), whereas, in the *matP* strain, condensation is altered and colocalization is looser and much shorter (vertical degraded gray bar). In both strains, replication initiation (green horizontal bar labeled R.I.) occurred in the mother cell. The Ter MD replication takes place in the daughter cells; the end of replication is marked by the red horizontal bar labeled R.E. The C period is represented by the green vertical bar. The rest of the chromosome is represented arbitrarily as unfolded (black/gray lines), and *oriC* is represented as a red dot.

that chromosome segregation in *E. coli* is a tightly controlled process. Not only does accurate transmission of chromosomes into daughter cells rely on early segregation of the Ori region, involving *migS* and MukBEF (Ohsumi et al., 2001; Yamaichi and Niki, 2004; Danilova et al., 2007), but our results also reveal that it requires a delay in Ter MD segregation, promoted by MatP. Upon completion of replication, duplicated MDs are kept together by MatP close to midcell (Figure 7). The size of the MatP focus is similar to that of the Ter MD territory, and, in more than 85% of the cells, markers of the Ter MD are localized in the MatP focus, suggesting that MatP contributes to the definition of the Ter MD cage. About 30 min before division, the Ter MDs individualize and segregate to daughter cells. The splitting of the MatP focus gives rise to two MatP foci concomitantly with the separation of the two Ter MDs. Initiation of Ter MD segregation might therefore be under the control of factor(s) that destabilize the MatP-dependent Ter MD colocalization either directly or indirectly, for example through the force applied to drive Ter MD segregation.

Chromosome Management at a Fast Growth Rate

Bacteria have the exceptional property of being able to drastically modify the cell-cycle parameters depending on growth conditions. The cell cycle of slowly growing *E. coli* cells is reminiscent of that of eukaryotic cells, with G1-, S-, and G2/M-like phases. However, in rich medium, the cell cycle is more complicated because the time it takes to replicate the chromosome can be longer than the generation time. Therefore, a new round of replication must be initiated before the previous round is completed. As a consequence, several overlapping replication cycles are under way in the same cell, and the topological complexity of the chromosome is increased. In this context, it is not surprising that Ter MD organization and condensation involving MatP is required under fast growth conditions, whereas it does not notably perturb cell physiology in slow growth conditions. A number of processes are already known to occur in the Ter MD; they include termination of replication (Coskun-Ari and Hill, 1997), decatenation of entangled chromosomes (Hojgaard et al., 1999), chromosome dimer resolution (Blakely et al., 1991), and coupling of replication with the cell cycle (Esnault et al., 2007). A challenge now is to identify the MatP-dependent process(es) required for proper chromosome management in rapidly growing cells.

Constraints on DNA Mobility by MatP

MDs defined genetically as insulated regions in the cell showed a limited mobility, whereas loci in NS regions exhibited a greater mobility (Espéli et al., 2008). MatP is the main factor restricting DNA mobility in Ter MD compared to mobility of NS regions. The cage sizes of the Ter MD markers in *matP* cells are comparable to those determined for NS region markers in WT cells. These results support a model whereby DNA in *E. coli* cells is constrained and the existence of two levels of DNA mobility would result from a limitation of the mobility in MDs rather than from a mobility increase in NS regions. Distinct DNA dynamics coexist in eukaryotic nuclei, and this is thought to reflect constraints exerted at different loci by nuclear substructures. Remarkably, the diffusion coefficients measured in *E. coli* are comparable to those obtained in eukaryotic cells (Mearini and Fackelmayer, 2006): in NS regions, the values are close to those obtained for loci located in the internal part of the nucleus (3.5×10^{-12} cm^2/s versus 3.7×10^{-12} cm^2/s), whereas in MDs, the values are similar to those of loci located at the nuclear periphery (1.5×10^{-12} cm^2/s versus 1.25×10^{-12} cm^2/s). Thus, we have shown that a DNA binding protein acting over a large distance modulates DNA dynamics. As observed in eukaryotes, we can rule out a role of gene activation in modulating DNA dynamics in *E. coli* because the transcriptome profiles of genes present in the Ter MD were not affected by MatP inactivation (R.M., F.B., and O.E., unpublished data). Our finding indicates that in NS regions and in the Ter MD in the absence of MatP, bulk chromosomal DNA in *E. coli* shows greater mobility. Interestingly, on the basis of the efficiency of site-specific recombination reactions, it was previously reported that the effective DNA concentration of plasmids in vivo is one order of magnitude lower than the chemical concentration (Hildebrandt and Cozzarelli, 1995). NAPs were proposed to be responsible for this effect since, as predicted for integration host factor (IHF) (Murtin et al., 1998),

they are thought to interact with most of the chromosomal DNA. The abundance of NAPs combined with their nonspecific binding and potent DNA bending activities could account not only for the reduction of the effective DNA concentration in the cell but also for the high mobility of the DNA molecule through rapid and unstable interactions. Characterization of the MatP interaction with Ter MD DNA and its influence on local chromatin composition will shed light on the parameters governing DNA mobility in prokaryotic cells.

EXPERIMENTAL PROCEDURES

Bacterial Strains, Plasmids, and Growth Conditions

E. coli K12 strains are all derivatives of MG1655. Standard growth, transformation, and transduction procedures used were as previously described (Valens et al., 2004). *parS* tags and antibiotic resistance genes were integrated as described before (Espéli et al., 2008). Plasmids and strains with relevant genotypes are described in Tables S3 and S4. The strains were grown in liquid Lennox medium at 30°C or 37°C, liquid minimal medium A supplemented with 0.1% casamino acids and 0.4% glucose at 30°C. The position of *parS* tags is indicated in Table S5.

Statistical Analysis

To evaluate the exceptionality of motif (hereafter called "word") frequencies, we used the R'MES software (http://genome.jouy.inra.fr/ssb/rmes/). Prior to statistical analysis, all repeats of a size greater than 40 bps were masked with the Vmatch software (http://www.vmatch.de/). Two files corresponding to the sequence of the Ter MD in *E. coli* MG1655 (coordinates 1,229,217 to 1,900,000, GenBank strand) and to the sequence of the *E. coli* MG1655 genome outside the Ter MD domain were generated. Words were considered together with their reverse-complementary sequence. We used the a posteriori prediction of the known *parS* site of *B. subtilis* in order to define two important parameters: the length of the words to be analyzed and the order of Markov chain used as a model for estimating expected counts of each word (Supplemental Experimental Procedures, Figure S8, and Table S7). Analyzing words of 11 bp with a Markovian model of order 5 (taking into account mono- to hexamer composition) allowed the identification of one of the *parS* submotifs as the most exceptional in the origin proximal domain of the *B. subtilis* genome. We therefore computed the exceptionality score for all 11 bp words of the Ter MD of *E. coli* with a Markovian model of order 5. In addition to this exceptionality criterion, a "contrast" criterion was used: words that were more exceptional inside the Ter MD were selected. For this, a binomial test was applied, determining whether the exceptionality of each of the 505,775 11-mers present at least once in the Ter MD was significantly higher inside than outside the domain (Robin et al., 2007). The ten most exceptional candidates in the Ter MD having a contrast p value below 5% are listed in Table S1, and, remarkably, six are overlapping.

Long-Range DNA Interactions

The recombination test measuring DNA collisions was performed as described previously (Valens et al., 2004). Because cells showed important growth defects in conditions used before (rich medium), recombination assays were performed in minimal medium and the recombinase expression was induced for 10 min at 38°C at OD$_{600}$ = 0.2.

Chromatin Immunoprecipitation

ChIP assays were performed as described (Danilova et al., 2007) with an affinity purified polyclonal antibody against MatP. Hybridization of Panorama gene arrays was performed with α^{32}P-dCTP-labeled probes generated by random priming of 50 ng of immunoprecipitated or total *E. coli* DNA.

Light and Fluorescence Microscopy

Microscopy observations were as described before (Espéli et al., 2008).

REFERENCES

Adachi, S., Fukushima, T., and Hiraga, S. (2008). Dynamic events of sister chromosomes in the cell cycle of *Escherichia coli*. Genes Cells *13*, 181–197.

Bates, D., and Kleckner, N. (2005). Chromosome and replisome dynamics in *E. coli*: loss of sister cohesion triggers global chromosome movement and mediates chromosome segregation. Cell *121*, 899–911.

Ben-Yehuda, S., Fujita, M., Liu, X.S., Gorbatyuk, B., Skoko, D., Yan, J., Marko, J.F., Liu, J.S., Eichenberger, P., Rudner, D.Z., and Losick, R. (2005). Defining a centromere-like element in *Bacillus subtilis* by Identifying the binding sites for the chromosome-anchoring protein RacA. Mol. Cell *17*, 773–782.

Blakely, G., Colloms, S., May, G., Burke, M., and Sherratt, D. (1991). *Escherichia coli* XerC recombinase is required for chromosomal segregation at cell division. New Biol. *3*, 789–798.

Brezellec, P., Hoebeke, M., Hiet, M.S., Pasek, S., and Ferat, J.L. (2006). DomainSieve: A protein domain-based screen that led to the identification of *dam*-associated genes with potential link to DNA maintenance. Bioinformatics *22*, 1935–1941.

Coskun-Ari, F.F., and Hill, T.M. (1997). Sequence-specific interactions in the Tus-Ter complex and the effect of base pair substitutions on arrest of DNA replication in *Escherichia coli*. J. Biol. Chem. *272*, 26448–26456.

Danilova, O., Reyes-Lamothe, R., Pinskaya, M., Sherratt, D., and Possoz, C. (2007). MukB colocalizes with the *oriC* region and is required for organization of the two *Escherichia coli* chromosome arms into separate cell halves. Mol. Microbiol. *65*, 1485–1492.

Esnault, E., Valens, M., Espeli, O., and Boccard, F. (2007). Chromosome structuring limits genome plasticity in *Escherichia coli*. PLoS Genet. *3*, e226.

Espéli, O., Mercier, R., and Boccard, F. (2008). DNA dynamics vary according to macrodomain topography in the *E. coli* chromosome. Mol. Microbiol. *68*, 1418–1427.

Guarne, A., Brendler, T., Zhao, Q., Ghirlando, R., Austin, S., and Yang, W. (2005). Crystal structure of a SeqA-N filament: implications for DNA replication and chromosome organization. EMBO J. *24*, 1502–1511.

Halpern, D., Chiapello, H., Schbath, S., Robin, S., Hennequet-Antier, C., Gruss, A., and El Karoui, M. (2007). Identification of DNA motifs implicated in maintenance of bacterial core genomes by predictive modeling. PLoS Genet *3*, 1614–1621.

Hildebrandt, E.R., and Cozzarelli, N.R. (1995). Comparison of recombination in vitro and in *E. coli* cells: measure of the effective concentration of DNA in vivo. Cell *81*, 331–340.

Hojgaard, A., Szerlong, H., Tabor, C., and Kuempel, P. (1999). Norfloxacin-induced DNA cleavage occurs at the dif resolvase locus in *Escherichia coli* and is the result of interaction with topoisomerase IV. Mol. Microbiol. *33*, 1027–1036.

Lee, P.S., Lin, D.C., Moriya, S., and Grossman, A.D. (2003). Effects of the chromosome partitioning protein Spo0J (ParB) on oriC positioning and replication initiation in *Bacillus subtilis*. J. Bacteriol. *185*, 1326–1337.

Li, Y., Youngren, B., Sergueev, K., and Austin, S. (2003). Segregation of the *Escherichia coli* chromosome terminus. Mol. Microbiol. *50*, 825–834.

Lin, D.C., and Grossman, A.D. (1998). Identification and characterization of a bacterial chromosome partitioning site. Cell *92*, 675–685.

Marston, A.L., and Errington, J. (1999). Dynamic movement of the ParA-like Soj protein of *B. subtilis* and its dual role in nucleoid organization and developmental regulation. Mol. Cell *4*, 673–682.

Mearini, G., and Fackelmayer, F.O. (2006). Local chromatin mobility is independent of transcriptional activity. Cell Cycle *5*, 1989–1995.

Murray, H., Ferreira, H., and Errington, J. (2006). The bacterial chromosome segregation protein Spo0J spreads along DNA from *parS* nucleation sites. Mol. Microbiol. *61*, 1352–1361.

Murtin, C., Engelhorn, M., Geiselmann, J., and Boccard, F. (1998). A quantitative UV laser footprinting analysis of the interaction of IHF with specific binding sites: Re-evaluation of the effective concentration of IHF in the cell. J. Mol. Biol. *284*, 949–961.

Nielsen, H.J., Li, Y., Youngren, B., Hansen, F.G., and Austin, S. (2006a). Progressive segregation of the *Escherichia coli* chromosome. Mol. Microbiol. *61*, 383–393.

Nielsen, H.J., Ottesen, J.R., Youngren, B., Austin, S.J., and Hansen, F.G. (2006b). The *Escherichia coli* chromosome is organized with the left and right chromosome arms in separate cell halves. Mol. Microbiol. *62*, 331–338.

Niki, H., Yamaichi, Y., and Hiraga, S. (2000). Dynamic organization of chromosomal DNA in *Escherichia coli*. Genes Dev. *14*, 212–223.

Ohsumi, K., Yamazoe, M., and Hiraga, S. (2001). Different localization of SeqA-bound nascent DNA clusters and MukF-MukE-MukB complex in *Escherichia coli* cells. Mol. Microbiol. *40*, 835–845.

Reyes-Lamothe, R., Possoz, C., Danilova, O., and Sherratt, D. (2008). Independent positioning and action of E*scherichia coli* replisomes in live cells. Cell *133*, 90–102.

Robin, S., Schbath, S., and Vandewalle, V. (2007). Statistical tests to compare motif count exceptionalities. BMC Bioinformatics *8*, 84.

Sunako, Y., Onogi, T., and Hiraga, S. (2001). Sister chromosome cohesion of *Escherichia coli*. Mol. Microbiol. *42*, 1233–1241.

Thanbichler, M., and Shapiro, L. (2006). Chromosome organization and segregation in bacteria. J. Struct. Biol. *156*, 292–303.

Valens, M., Penaud, S., Rossignol, M., Cornet, F., and Boccard, F. (2004). Macrodomain organization of the *Escherichia coli* chromosome. EMBO J. *23*, 4330–4341.

Viollier, P.H., Thanbichler, M., McGrath, P.T., West, L., Meewan, M., McAdams, H.H., and Shapiro, L. (2004). Rapid and sequential movement of individual chromosomal loci to specific subcellular locations during bacterial DNA replication. Proc. Natl. Acad. Sci. USA *101*, 9257–9262.

Wang, X., Possoz, C., and Sherratt, D.J. (2005). Dancing around the divisome: asymmetric chromosome segregation in *Escherichia coli*. Genes Dev. *19*, 2367–2377.

Wang, X., Liu, X., Possoz, C., and Sherratt, D.J. (2006). The two *Escherichia coli* chromosome arms locate to separate cell halves. Genes Dev. *20*, 1727–1731.

Yamaichi, Y., and Niki, H. (2004). *migS*, a cis-acting site that affects bipolar positioning of *oriC* on the *Escherichia coli* chromosome. EMBO J. *23*, 221–233.